JOURNAL
OF THE AMERICAN CHEMICAL SOCIETY

VOLUME 99, NUMBER 26 DECEMBER 21, 1977

Directional Effects of σ Conjugation on Geometrical Isomerism

Nicolaos D. Epiotis,*[1a] Ronald L. Yates,[1a] J. R. Larson,[1a] Christine R. Kirmaier,[1a] and Fernando Bernardi*[1b]

Contribution from the Department of Chemistry, University of Washington, Seattle, Washington 98195, and Istituto di Chimica Organica, Universita di Bologna, 40136 Bologna, Italy.

Received August 13, 1976

Abstract: The preferred geometry of many molecules can be viewed as the result of the maximization of an interaction between the best donor lone pair or bond and the best acceptor bond, i.e., the bond with the lowest lying antibonding orbital. The magnitude of this aforementioned "hyperconjugative" interaction is a function of the geometry of the interacting fragments. The anti rather than the syn orientation affords the maximal lone-pair-bond and/or bond-bond σ conjugative interactions. Ab initio calculations are employed to test the model and to probe the importance of "directive" σ conjugation relative to nonbonded attractive and steric effects in diverse molecular systems.

Interactions between orbitals can be stabilizing or destabilizing depending upon orbital occupancy. In general, the interaction between an occupied and an unoccupied orbital is stabilizing, the dependence of the stabilization given by the expression[2,3]

$$\mathrm{SE} \propto \frac{S^2}{\Delta E} \qquad (1)$$

where S is the overlap integral of the two interacting orbitals and ΔE their energy separation. Such stabilizing interactions can be of the π–π^*, n–π^*, π–σ^*, σ–π^*, n–σ^*, and σ–σ^* variety, where the asterisk denotes an antibonding vacant orbital and the absence of an asterisk implies a bonding, doubly occupied orbital. On the other hand, the interaction between two occupied orbitals is destabilizing. Destabilizing interactions play a definite role in determining geometrical preferences, but, since we strive for the simplest possible qualitative model, we shall neglect them. This assumption is based on the general experience[4] that two-electron stabilizing interactions are more important than four-electron destabilizing interactions. Accordingly, we shall focus our attention on the former interactions and how they determine geometrical preferences. We shall distinguish between π conjugative interactions (π–π^*) and σ conjugative interactions, otherwise referred to as hyperconjugative interactions, of the n–π^*, π–σ^*, σ–π^*, n–σ^*, and σ–σ^* type. Interactions of the n–π^* type can be understood on the basis of simple resonance theory, while interactions of the π–σ^* and σ–π^* type have been discussed by various authors.[5-7] In this paper we shall be concerned about n–σ^* and σ–σ^* interactions which, unlike n–π^* and π–σ^* interactions, display strong directional preferences. The contribution of this paper is to point out how these directional preferences may be responsible for the relative stability of geometric isomers.

Theory

In our subsequent discussions, we shall be using hybrid lone pair AOs and hybrid bond MOs. The explicit forms of these orbitals are given below for the case of any lone pair located on atom Y and the case of an X–H bond:

$$n_Y = h_Y(\mathrm{sp}^2) \text{ or } n_Y = h_Y(\mathrm{sp}^3)$$

$$\sigma_{X-H} = h_X(\mathrm{sp}^2) + \lambda 1s_H \text{ or } \sigma_{X-H} = h_X(\mathrm{sp}^3) + \lambda 1s_H$$

$$\sigma^*_{X-H} = h_X(\mathrm{sp}^2) - \lambda 1s_H \text{ or } \sigma^*_{X-H} = h_X(\mathrm{sp}^3) - \lambda 1s_H$$

The hybrid sp^2 and sp^3 AOs can be simply written in terms of s and p AOs as follows:[8]

$$h(\mathrm{sp}^2) = 0.577\mathrm{s} + 0.408\mathrm{p}_x + 0.707\mathrm{p}_y$$

$$h(\mathrm{sp}^3) = 0.500\mathrm{s} + 0.288\mathrm{p}_x + 0.816\mathrm{p}_y$$

An important point to be stressed is the formal correspondence between hybrid orbitals and delocalized group orbitals. For example, consider the model system fragment $\mathrm{H\ddot{N}}$–.

The group MOs for $\mathrm{H\ddot{N}}$– are depicted in Figure 1a.[9] The sp^2 hybrid lone pair AO on nitrogen and the corresponding N–H σ and σ^* MOs, made up of an sp^2 hybrid nitrogen AO and a hydrogen 1s AO, are shown in Figure 1b. Obviously, ϕ_1, ϕ_2, and ϕ_3 are essentially a σ_{N-H} MO, an sp^2 lone pair AO, and a σ^*_{N-H} MO, respectively.

The next step is to consider the factors which enhance or diminish n–σ^* and σ–σ^* conjugative interactions. These are as follows.

(a) *The energy separation factor* ΔE. As ΔE decreases, i.e., as the ionization potential of n or σ decreases and the electron affinity of σ^* increases, conjugative interactions become stronger. The energy factor provides the index for isolating the

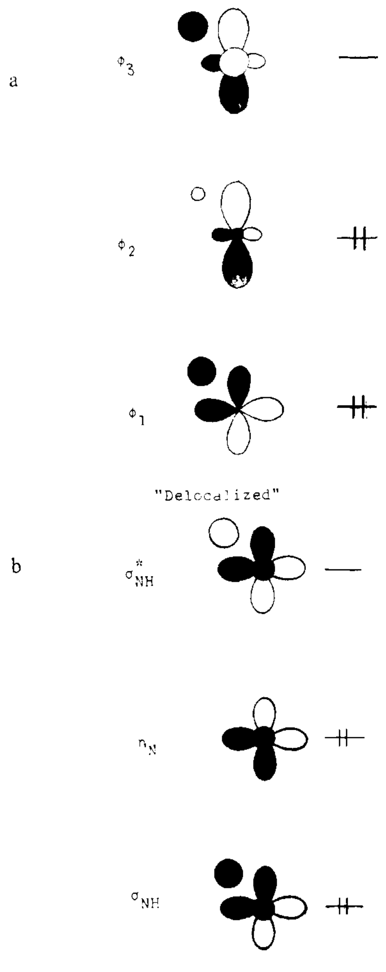

Figure 1. (a) Delocalized MOs of the $H\ddot{N}$- fragment. Relative magnitudes of the AO coefficients were taken from a CNDO/2 calculation. (b) MOs of the $H\ddot{N}$- fragment assuming that N is sp^2 hybridized.

dominantly interacting fragments. In general, the energy of a lone pair MO increases as atom electronegativity decreases and the energy of a σ_{X-Y} bonding MO increases as the electronegativity of Y decreases. In addition, the energy of a σ_{X-Y} antibonding MO decreases as the electronegativity of Y increases along a row or decreases along a column of the periodic table.[4b]

(b) *The overlap factor.* As S increases, conjugative interactions become stronger. The overlap factor provides *the index for choosing the preferred geometry of two dominantly interacting fragments.*

Since our theoretical predictions will be compared with experimental results as well as explicit quantum mechanical calculations, it is important to define a theoretical quantity which reflects the strength of n-σ^* and σ-σ^* conjugative interactions. Since these interactions give rise to charge transfer from n to σ^* or from σ to σ^*, one can easily identify an increasingly strong σ conjugative interaction from an observation of greater charge depletion of the donor orbital (n or σ) and a greater charge accumulation in the acceptor (σ^*) orbital. Accordingly, atomic charges obtained from calculations will be interpreted along these lines.

In addition to the above index, the geometry of a molecule, as obtained from calculation by optimizing all, or most, structural parameters, should provide us with an indication of the importance of σ conjugative interactions. Thus, charge transfer from an n to σ^* should result in lengthening of the acceptor bond while charge transfer from σ to σ^* should result in lengthening of both donor and acceptor bonds. Of course, the effects of charge transfer can also be revealed by an examination of atom-atom overlap populations which, in general, parallel bond lengths.

The above discussion provides the necessary background. We now enter into the discussion of the key problem that we shall be concerned with. For example, consider the $H\ddot{N}=\ddot{N}H$ model system shown below. In the cis geometry there are two syn σ-σ^* interaction and two anti n-σ^* interactions, while in the trans geometry there are two anti σ-σ^* interactions and two syn n-σ^* interactions. Now, a lone pair has higher energy than a bonding σ MO, or, in other words, the nitrogen lone pair is a better donor fragment than N-H. Hence, we focus attention on the dominant interaction between the best donor orbital n_N and the best acceptor orbital σ^*_{NH}. The stabilization energy difference for the cis and trans geometries due to the n_N-σ^*_{NH} interaction is approximated by the expression

$$SE_{cis} - SE_{trans} \propto \frac{1}{\Delta E}(S^2_{anti} - S^2_{syn})$$

We need to evaluate the overlap integrals S_{anti} and S_{syn}, pictured in Figure 3 in both their hybrid and expanded forms, in order to determine which of the two geometries is favored. This is a fundamental problem in geometric or conformational isomerism. Fortunately, a general rule allows the qualitative prediction of the relative size of syn and anti overlap integrals between n and σ^* or σ and σ^*.

The n-σ^* overlap integrals for the syn and anti arrangements in HN=NH are given below. In these equations the AO overlap integrals are all taken as positive and the sign of each term is determined from consideration of the phases of the overlapping AOs as shown in Figure 2.

$$S_{syn} \propto Q + (0.707)^2(p_y|p_{y'}) - \lambda(0.707)(1s|p_{y'}) \quad (2)$$

$$S_{anti} \propto Q - (0.707)^2(p_y|p_{y'}) + \lambda(0.707)(1s|p_{y'}) \quad (3)$$

where Q is constant for both cases and is given by the expression

$$Q = (0.577)^2(s|s) - (0.577)(0.408)(s|p_x) - (0.408)(0.577)(p_x|s) + (0.408)^2(p_x|p_x) - \lambda(0.577)(1s|s) + \lambda(0.408)(1s|p_x) \quad (4)$$

In general, Q is a negative number.

Equations 2 and 3 are reduced to the form

$$S_{syn} = -|Q| + |R| \quad (2')$$

$$S_{anti} = -|Q| - |R| \quad (3')$$

where R is defined as

$$R = [(0.707)^2(p_y|p_{y'}) - \lambda(0.707)(1s|p_{y'})] \quad (5)$$

The important points to be emphasized here are that (a) the invariant quantity Q is negative; (b) the variable quantity R will always be negative for the anti geometry and positive for the syn geometry owing to the dominance of the p_y-$p_{y'}$ overlap.

Table I shows calculated overlap integrals for various combinations of hybridized atomic centers. In all cases, the difference in the absolute magnitude is $2Q$ favoring greater overlap in the cis geometry.

We can work in a similar manner to examine the relative absolute magnitudes of syn and anti overlaps for σ-σ^* interaction. The two arrangements are depicted in Figure 3 and we

Table I. $\langle n|\sigma^*\rangle$ Overlap Integrals

Interacting orbitals	Overlap integrals[a] Syn overlap (trans isomer)	Anti overlap (cis isomer)	Δ[b]
$\langle n_{Nsp^2}\|\sigma^*_{HNsp^2}\rangle$	0.0357	0.0867	0.0510
$\langle n_{Nsp^3}\|\sigma^*_{HNsp^3}\rangle$	0.0251	0.0623	0.0372
$\langle n_{Nsp^2}\|\sigma^*_{HNsp^2}\rangle$	0.0567	0.0977	0.0410
$\langle n_{Nsp^3}\|\sigma^*_{HNsp^3}\rangle$	0.0554	0.0840	0.0286
$\langle n_{Csp^2}\|\sigma^*_{HNsp^2}\rangle$	0.0321	0.0817	0.0496
$\langle n_{Csp^3}\|\sigma^*_{HNsp^3}\rangle$	0.0243	0.0677	0.0434
$\langle n_{Csp^2}\|\sigma^*_{HCsp^2}\rangle$	0.0689	0.1173	0.0484
$\langle n_{Csp^3}\|\sigma^*_{HCsp^3}\rangle$	0.0570	0.0874	0.0304

[a] AO overlap integrals were taken from CNDO/2 calculations. [b] $\Delta = |S_{anti}| - |S_{syn}| = 2|Q|$.

Table II. $\langle\sigma|\sigma^*\rangle$ Overlap Integrals

Interacting orbitals	Overlap integrals[a] Syn	Anti
$\langle\sigma_{NHsp^2}\|\sigma^*_{NHsp^2}\rangle$	0.0076	0.1420
$\langle\sigma_{NHsp^3}\|\sigma^*_{NHsp^3}\rangle$	0.0166	0.1176
$\langle\sigma_{CHsp^2}\|\sigma^*_{NHsp^2}\rangle$	0.0066	0.1271
$\langle\sigma_{CHsp^3}\|\sigma^*_{NHsp^3}\rangle$	0.0161	0.1176
$\langle\sigma_{NHsp^2}\|\sigma^*_{CHsp^2}\rangle$	0.0555	0.1592
$\langle\sigma_{NHsp^3}\|\sigma^*_{CHsp^3}\rangle$	0.0461	0.1500
$\langle\sigma_{CHsp^2}\|\sigma^*_{CHsp^2}\rangle$	0.0667	0.1799
$\langle\sigma_{CHsp^3}\|\sigma^*_{CHsp^3}\rangle$	0.0472	0.1437

[a] AO overlaps were taken from CNDO/2 calculations.

obtain the following equations:

$$S_{syn} \propto Q + R - M \tag{6}$$

$$S_{anti} \propto Q - R - N \tag{7}$$

where

$$\begin{aligned} Q = {} & (0.577)^2(s|s) - (0.577)(0.408)(s|p_x) \\ & - (0.408)(0.577)(p_x|s) + (0.408)^2(p_x|p_x) \\ & - \lambda(0.577)(1s|s) + \lambda(0.408)(1s|p_x) \end{aligned} \tag{8}$$

$$R = [(0.707)^2(p_y|p_y) - \lambda(0.707)(1s|p_y)] \tag{9}$$

$$M = \lambda^2(1s|1s) \tag{10}$$

$$N = \lambda^2(1s|1s) \tag{11}$$

In this case the invariant term Q can be either positive or negative simply because a strong bonding X-H overlap at one site is counteracted by a strong antibonding X-H overlap at the other site and the remaining terms can sum to either a positive or negative number depending on interatomic distances. Either way, the absolute magnitude of Q is much smaller than any of the terms R, M, or N. R and M are close in magnitude with R usually, but not always, being the larger. In the case of syn overlap R and M tend to cancel each other, so that a small value for the overlap integral is obtained. R and N reinforce each other in the case of anti overlap, the result being that S_{anti} is greater in absolute magnitude than S_{syn}. Typical computed overlap integrals are collected in Table II.

The Prediction of Geometry, Gross Atomic Charges, and Bond Overlap Population. We are now prepared to state a general "recipe" for the prediction of geometrical preferences assuming that the key effect which determines such preferences is a σ conjugative effect. Our conclusions would have to be modified if other effects, such as nonbonded attraction or repulsion, are also present. The steps that should be taken when attempting a prediction are the following:

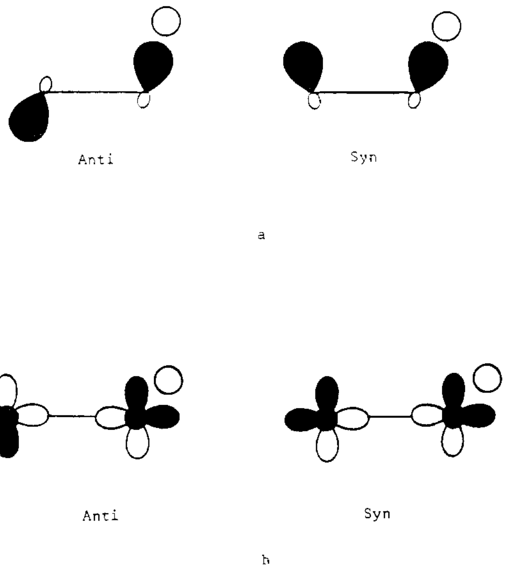

Figure 2. Pictorial representation of the overlap integrals S_{anti} and S_{syn} for an n_y-σ^*_{XH} interaction in both the (a) hybrid and (b) expanded forms.

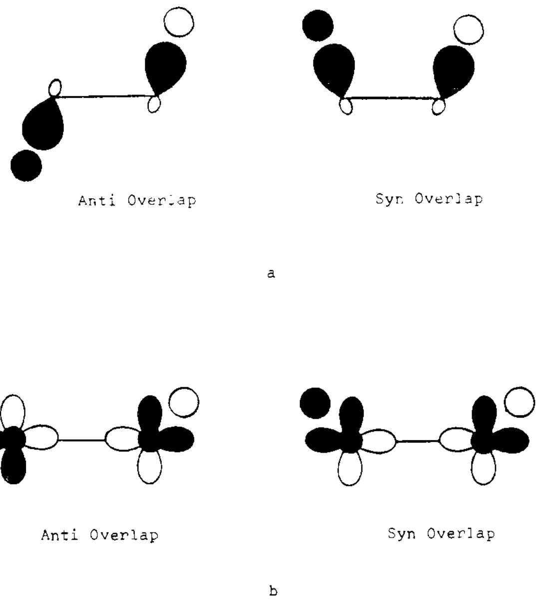

Figure 3. Pictorial representation of the overlap integrals S_{anti} and S_{syn} for a σ_{XH}-σ^*_{XH} interaction in both the (a) hybrid and (b) expanded forms.

(a) Identify the fragments which are capable of interacting in a dominant fashion, i.e., select the best donor lone pair or bond and the best acceptor bond (the bond with the lowest antibonding orbital). In most problems of interest, n-σ^* interactions will be more important than σ-σ^* interactions since the energy gap separating n and σ^* orbitals is, in general, much smaller than that separating σ and σ^* orbitals.

(b) The geometry which places the two bonds (the donor bond or lone pair and the acceptor bond) anti to each other will be preferred.

In discussing gross atomic charges it must be realized that a given pattern of atomic charge densities in a molecule can arise from several factors. We identify three effects responsible for a molecular charge distribution: (1) σ conjugative effects; (2) nonbonded interactive effects; (3) electrostatic effects.

The mechanism of charge reorganization attending the interconversion of geometric isomers due to nonbonded interaction effects has already been discussed in earlier publications.[15-20] The electrostatic effect can be thought of as an effect

Table III. Geometrical Parameters and Total Energies[a] of N_2H_2

	Cis	Trans
r(N-N), Å	1.264	1.267
r(N-H), Å	1.064	1.061
∠H-N-N	111.50°	105.30°
E_T(STO-3G), au	−108.545 24	−108.556 95
E_T(4-31G), au	−109.792 51[b]	−109.805 25[b]

[a] W. A. Lathan, L. A. Curtiss, W. J. Hehre, J. B. Lisle, and J. A. Pople, *Prog. Phys. Org. Chem.*, **11**, 175 (1974). [b] Energy is computed at the STO-3G optimized geometry.

which forces the distribution of charge in such a way that electrostatic repulsions will be minimized.

As an example, let us consider cases of N_2H_2 and N_2F_2. If σ conjugative interactions were the dominant factor, then we would predict that the cis hydrogens should be less positive than the trans hydrogens since charge transfer from n_N to σ^*_{N-H} is greater in the cis isomer. Based solely on electrostatic considerations, one would also predict less positive charge on the cis rather than the trans hydrogens in order to minimize the repulsive H—H interaction which is more severe in the cis than in the trans isomer. In the case of N_2F_2, the nonbonded interaction effect predicts that the fluorines in the cis isomer will be less negative than in the trans isomer because of greater charge transfer from antisymmetric F—F π and σ group MOs into antibonding π and σ group MOs of the N=N moiety having appropriate symmetry. A similar prediction is made on the basis of electrostatic effects. However, if a σ conjugative interaction is the dominant factor, then the cis fluorines should be more negative than the fluorines in the trans isomer.

In light of the above two examples it is imperative that caution be exercised in the interpretation of charge densities in terms of one effect only. A comparison of calculated charge densities with those predicted by the three approaches will be useful in some cases in pinpointing the factor primarily responsible for the stability of a certain geometric isomer.

These same factors determine bond overlap populations. Once more, let us consider the case of N_2F_2. If the σ conjugative effect is dominant, we expect the N-F overlap population to be smaller in the cis isomer where the n_N-σ^*_{NF} interaction is maximized. On the other hand, if the nonbonded interaction effect is dominant, we expect exactly the opposite trend, i.e., larger N-F overlap population in the cis isomer, owing to a stronger mixing of the antisymmetric F···F π group MO with the antibonding π group MO of the N=N moiety. Finally, a steric effect cannot lead to the prediction of smaller N-F overlap population in the more "crowded" cis isomer.

Following similar reasoning, we predict that the N=N bond overlap population will be smaller in the cis isomer if steric effects or nonbonded interaction effects obtain and larger if σ conjugative effects dominate.

Results

We have chosen to investigate by means of ab initio quantum mechanical calculations systems of the following types:

(a) $R\ddot{N}{=}\ddot{N}R$ systems. In these molecules, dominant n-σ^* interactions will tend to favor a cis geometry.

(b) $RCH{=}\ddot{N}R$ and $RCH{=}\ddot{C}R^-$ systems. In these molecules, dominant n-σ^* interactions will tend to favor a cis geometry.

(c) RCH=CHR systems. In these molecules, only σ-σ^* interactions are possible and the preference should be small. Other effects such as nonbonded attractive effects could dominate here.

Thi ab initio computations were performed using the GAUSSIAN 70 series of programs.[21] In all cases, geometry optimization was carried out using the STO-3G basis set.[22] In some cases, geometry optimization was also carried out using the extended 4-31G basis set.[23]

The optimized geometries and the total energies are given in Tables III-IX. Some of the ab initio data is presented in the various schemes in the following manner: atomic charges are placed next to atoms (in parentheses) and total bond overlap populations between the appropriate atoms. Furthermore, total π overlap populations, $N_T{}^\pi$, long-range π overlap populations between two X atoms, $P_{XX}{}^\pi$, and long-range σ overlap populations between two X atoms, $P_{XX}{}^\sigma$, are given for each geometric isomer. These latter quantities constitute indexes of nonbonded X···X attraction.

A. $R\ddot{N}{=}\ddot{N}R$ Systems. The parent system HN=NH[24a] can exist in the cis and trans geometries. We have already discussed the fact that the n_N-σ^*_{NH} interactions will tend to bias N_2H_2 toward cis preference which is predicted to increase upon replacement of H by F.

The relative energies, atomic charges, and bond overlap populations of *cis*- and *trans*-N_2H_2 are shown in Scheme I.

Scheme I.

4-31G Calculation at STO-3G Optimized Geometry (See Table III)

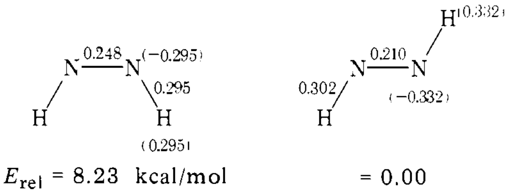

The relative magnitude of charge, overlap population, and total energies of the geometric isomers of N_2H_2 as predicted on the basis of each of the three important effects thought to determine molecular structure are shown in Table X. Comparison of the ab initio data with the various predictions reveals that σ conjugative effects are larger in the cis isomer, i.e., the N=N overlap population varies in the order cis > trans. However, the trans isomer is found to be more stable than the cis isomer. Thus, we conclude that geometric isomerism in N_2H_2 is dominated by steric effects.

The ab initia data for N_2F_2 are displayed in Scheme II and predictions based on considerations of each of the three effects previously discussed are presented in Table XI. Comparison of the ab initio and experimental data with the various pre-

Table IV. Geometrical Parameters and Total Energies of *cis*- and *trans*-N_2F_2 Computed at the STO-3G Level

	STO-3G		Exptl[a]	
	Cis	Trans	Cis	Trans
r(N-N), Å	1.2897	1.2621	1.214	1.231
r(N-F), Å	1.3772	1.3728	1.410	1.396
∠F-N-N	111.61°	106.62°	114.4°	105.5°
E_T(STO-3G), au	−303.440 67	−303.440 20		
E_T(4-31G), au	−307.133 97[b]	−307.138 32[b]		

[a] See ref 25. [b] Energy values computed at the STO-3G optimized geometry.

Table V. Total Energies and Geometrical Parameters for I Computed at the STO-3G Level

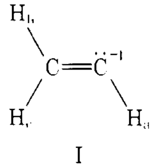

I

r(C-C), Å	1.3275
r(C-H$_c$), Å	1.0953
r(C$_1$-H$_b$), Å	1.0845
r(C$_2$-H$_a$), Å	1.1164
∠H$_b$CC	125.27°
∠H$_c$CC	127.45°
∠CCH$_a$	105.69°
E_T(STO-3G), au	−76.232 47
E_T(4-31G), au	−77.212 15[a]

[a] Energy value computed at the STO-3G optimized geometry.

Scheme II

A. STO-3G Calculation at STO-3G Geometry (See Table IV)

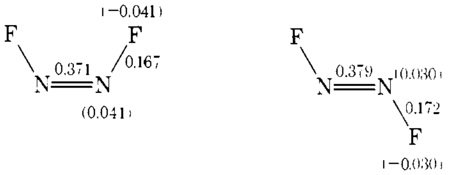

E_{rel}, kcal/mol	0.000	0.634
$N_T{}^{\pi}$	0.170 57	0.175 20
$P_{FF}{}^{\pi}$	0.000 15	0.000 00
$P_{FF}{}^{\sigma}$	−0.000 16	0.000 00

B. 4-31G Calculation at STO-3G Geometry (See Table IV)

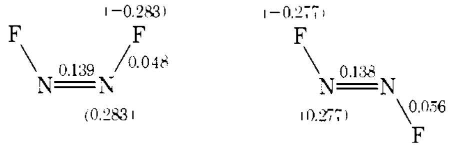

E_{rel}, kcal/mol	2.535 (0.000)[24b]	0.000 (1.047)[24b]
$N_T{}^{\pi}$	0.183 17	0.179 59
$P_{FF}{}^{\pi}$	0.001 15	0.000 02
$P_{FF}{}^{\sigma}$	0.000 03	0.000 09

dictions reveals that σ conjugative effects are consistent with all ab initio and experimental data. Two slight anomalies are noted. First, the relative N=N overlap populations in the two isomers varies depending upon the basis set. The extended basis set yields results consistent with expectations based on consideration of σ conjugative effects. Second, the STO-3G basis set predicts greater stability of the cis isomer, in agreement with experimental results,[25] while 4-31G predicts the opposite. However, geometry optimization at the 4-31G level correctly predicts that the cis isomer is preferred.[24b]

An interesting question arises: does the greater lengthening of the N-F bond in the cis isomer (vide infra) render the attractive π nonbonded interaction between the two fluorines in this isomer insignificant? The STO-3G results seem to suggest that this is true since total π overlap population, $N_T{}^{\pi}$, is greater for the trans isomer indicating that loss in N-F π overlap is the controlling influence of the relative π stabilization of the two geometric isomers. By contrast, the 4-31G results suggest that despite the larger N-F bond in the cis isomer, π nonbonded attraction still favors the cis isomer significantly. Thus, the difference in the total π overlap populations of the cis and trans isomers of N_2F_2 is substantial in favoring the cis isomer. Accordingly, it is not possible to draw a clear answer regarding the relative importance of σ conjugative and π nonbonded interaction effects. σ nonbonded interaction effects appear to be small and, in fact, favor the trans isomer because the vacant σ MOs of the $\ddot{N}=\ddot{N}$ unit act collectively as an effective symmetrical level.[4b]

An interesting "theoretical experiment" was performed by Howell et al., who gradually increased the nuclear charge of H in N_2H_2 and reduced the nuclear charge of N by a comparable amount, thus making the $\ddot{N}H^-$ fragment an increasingly better acceptor.[26] According to our analysis such progressive modification should lead to increasing strength of n-σ* interaction and a greater preference for the cis geometry in $H'-\ddot{N}'=\ddot{N}'H'$. This is exactly what these workers found.

B. RCH=$\ddot{N}$R Systems. In the parent system shown below, the strength of the various σ interactions varies in the order

$$n_N-\sigma^*_{CH_c}\ (\text{anti}) > n_N-\sigma^*_{CH_b}\ (\text{syn}) > \sigma_{CH_b}-\sigma^*_{NH_a}\ (\text{anti})$$

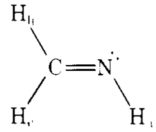

Table VI. Total Energies and Geometrical Parameters for $F_bCH=C^-F_a$ Computed at the STO-3G Level

	Geometry	
	Cis	Trans
r(C-C$_2$), Å	1.3342	1.3305
r(C-F$_b$), Å	1.4091	1.3876
r(C-H), Å	1.0909	1.0947
r(C-F$_a$), Å	1.3867	1.3865
∠HCC	120.40°	127.60°
∠F$_b$CC	131.01°	123.11°
∠CCF$_a$	110.93°	101.28°
E_T(STO-3G), au	−271.193 47	−271.192 95
E_T(4-31G), au	−274.726 58[a]	−274.726 10[a]

[a] Energy values computed at the STO-3G optimized geometry.

Table VII. Total Energies and Geometrical Parameters[a] for II Computed at the STO-3G Level

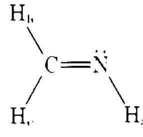

II

r(C-N), Å	1.274
r(C-H$_c$), Å	1.091
r(N-H$_a$), Å	1.049
r(C-H$_b$), Å	1.089
∠H$_b$CN	119.0°
∠H$_c$CN	125.0°
∠CNH$_a$	109.0°
E_T(STO-3G), au	−92.823 03
E_T(4-31G), au	−93.879 36[b]

[a] The STO-3G total energy and geometrical parameters were taken from ref 27. [b] Energy values computed at the STO-3G optimized geometry.

Scheme III. 4-31G Calculation at STO-3G Geometry (See Table VII)

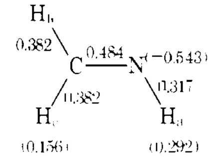

Table VIII. Computed Total Energies and Geometrical Parameters for $HCF_b{=}\ddot{N}F_a$

	Geometry			
	Cis		Trans	
	STO-3G	4-31G	STO-3G	4-31G
r(C-N), Å	1.291	1.2469	1.291	1.2419
r(C-F_b), Å	1.347	1.3368	1.344	1.3352
r(N-F_a), Å	1.379	1.4186	1.378	1.4174
r(C-H), Å	1.094	1.0635	1.098	1.0638
∠HCN	119.0°	119.64°	120.0°	126.53°
∠F_bCN	124.0°	125.67°	125.0°	118.87°
∠CNF_a	111.0°	111.10°	109.0°	107.41°
E_T(STO-3G), au	−287.720 19		−287.718 84	
E_T(4-31G), au	−291.271 54[a]	−291.275 97	−291.270 27[a]	−291.275 35

[a] Energy is computed at the STO-3G optimized geometry.

Table IX. Geometrical Parameters and Total Energies of *cis*- and *trans*-FHC=CHF Computed at the STO-3G Level

	STO-3G		Exptl[a]	
	Cis	Trans	Cis	Trans
r(C-C), Å	1.3264	1.3256	1.331	1.329
r(C-F), Å	1.3581	3.3572	1.335	1.344
r(C-H), Å	1.07[b]	1.07[b]	1.084	1.080
∠FCC	124.20°	122.97°	123.72°	119.33°
∠HCC	120.52°	121.89°	121.56°	129.25°
E_T(STO-3G), au	−271.984 92	−271.985 31		
E_T(4-31G), au	−275.366 03[c]	−275.366 86[c]		

[a] See ref 30. [b] C-H bond lengths were not optimized. [c] Energy values computed at the STO-3G optimized geometry.

Table X. Predicted Charges, Overlap Populations, and Relative Stability of the Geometric Isomers of N_2H_2

Property	σ conjugative effect	Nonbonded interaction effect	Electrostatic or steric effect	Ab initio
H positive charge	Trans > cis		Trans > cis	Trans > cis
N-H overlap population	Trans > cis		Trans > cis	Trans > cis
N=N overlap population	Cis > trans		Trans > cis	Cis > trans
Relative stability	Cis > trans		Trans > cis	Trans > cis

Table XI. Predicted Charges, Overlap Populations, and Relative Stability of the Geometric Isomers of N_2F_2

Property	σ conjugative effect	Nonbonded interaction effect	Electrostatic or steric effect	Ab initio
F negative charge	Cis > trans	Trans > cis	Trans > cis	Cis > trans
N-F overlap population	Trans > cis	Cis > trans	Trans > cis	Trans > cis
N=N overlap population	Cis > trans	Trans > cis	Trans > cis	Cis > trans[a] Trans > cis[b]
Relative stability	Cis > trans	Cis > trans	Trans > cis	Cis > trans[b] Trans > cis[a]

[a] 4-31G basis set. [b] STO-3G basis set.

Accordingly, if σ conjugative effects dominate, the hydrogen atoms are predicted to become increasingly positive in the order $H_c < H_b$ and the C-H overlap populations to vary in the order C-H_c < C-H_b.

The various atomic charges and bond overlap populations of $CH_2{=}\ddot{N}H$ are shown below and confirm an expectation based on consideration of σ conjugative effects. An anomaly is noted in the case of the 4-31G calculation of the C-H_b and C-H_c overlap populations. However, the STO-3G optimization does lead to a longer C-H_c bond, as predicted (see Table VII).

Accordingly, these intramolecular comparisons where σ conjugative effects are not pitted against other important effects provide good evidence of the superiority of anti orbital overlap.

The ab initio data for $CHF{=}\ddot{N}F$ are displayed in Scheme IV and predictions based on consideration of each of the three important effects previously discussed are collected in Table XII.

Comparison of the ab initio data with the various predictions reveals that F···F nonbonded interaction absolutely dominates geometric isomerism in $CHF{=}\ddot{N}F$. The large difference in the total π overlap populations and long-range diatomic overlap populations between the cis and trans isomers (Scheme IV) provides yet another demonstration of the importance of nonbonded interaction in determining structure.

The importance of σ conjugative interactions can be realized by restricting ourselves to intramolecular comparisons. The order of strength of σ conjugative interactions is $n_N\text{-}\sigma^*_{CF_b} > n_N\text{-}\sigma^*_{CH} > \sigma_{CH}\text{-}\sigma^*_{NF_a}$ and thus we predict that within a given isomer F_a should be less negative than F_b, as exactly revealed in the ab initio calculation. Once again, these data provide support for the idea that syn and anti orbital overlap lead to widely differing stabilization.[27]

Table XII. Predicted Charges, Overlap Populations, and Relative Stability of the Geometric Isomers $CHF_b{=}NF_a$

Property	σ effect	Nonbonded effect	Electrostatic or steric effect	Ab initio
H positive charge	Cis > trans		Trans > cis	Cis > trans
F_a negative charge	Cis > trans	Trans > cis	Trans > cis	Trans > cis
F_b negative charge	Cis > trans	Trans > cis	Trans > cis	Trans > cis
C–F overlap population	Trans > cis	Cis > trans	Trans > cis	Cis > trans
N–F overlap population	Trans > cis	Cis > trans	Trans > cis	Cis > trans
C=N overlap population	Cis > trans	Trans > cis	Trans > cis	Trans > cis
Relative stability	Cis > trans	Cis > trans	Trans > cis	Cis > trans

Scheme IV

A. 4-31G Calculation of STO-3G Geometry (See Table VIII)

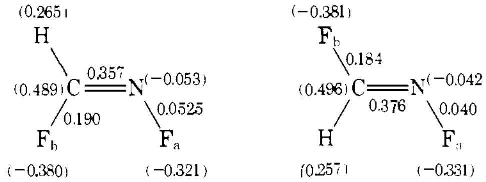

E_{rel}, kcal/mol	0.000	0.796
$N_T{}^{\pi}$	0.194 89	0.191 04
$P_{FF}{}^{\pi}$	0.000 63	0.000 01
$P_{FF}{}^{\sigma}$	0.000 04	0.000 08

B. 4-31G Calculation at 4-31G Geometry (See Table VIII).

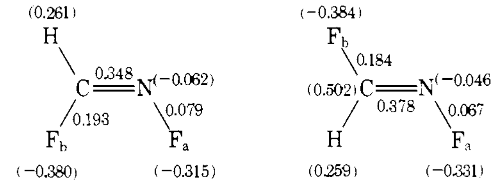

E_{rel}, kcal/mol	0.000	0.634
$N_T{}^{\pi}$	0.207 55	0.202 34
$P_{FF}{}^{\pi}$	0.000 53	0.000 01
$P_{FF}{}^{\sigma}$	0.000 01	0.000 08

C. $RCH{=}\ddot{C}R^-$ Systems. In the parent system shown below, the strength of the various σ interactions varies in the order

$$n_C-\sigma^*{}_{CH_c}\ (\text{anti}) > n_C-\sigma^*{}_{CH_b}\ (\text{syn}) > \sigma_{CH_b}-\sigma^*{}_{CH_a}\ (\text{anti})$$

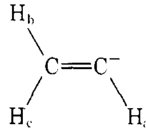

By following the same analysis in the case of $CH_2{=}NH$, we predict increases in charge density in the order $H_c > H_b$ as well as increasing overlap population in the order $C{-}H_b > C{-}H_c$. These predictions are confirmed, for the most part, by the ab initio results shown in Scheme V. The only anomaly is the basis set dependence of the relative $C{-}H_b$ and $C{-}H_c$ overlap populations.

The ab initio data for $CHF{=}CH^-$ are displayed in Scheme VI. The predictions based on consideration of each of the three key effects previously discussed are identical with those for $CHF{=}\ddot{N}F$. A comparison of the predictions with the calculation data shows unequivocally that $CHF{=}\ddot{C}F^-$ behaves exactly like its isoelectronic analogue $CHF{=}NF$ insofar as geometric isomerism is concerned, i.e., the relative energy of the cis and trans isomers of $CHF{=}\ddot{C}F^-$ is dominated by F···F nonbonded attraction. Intermolecular comparisons of fluorine charge densities are consistent with the trend expected on the basis of σ conjugation.

Scheme V

A. STO-3G Calculation at STO-3G Geometry (See Table V)

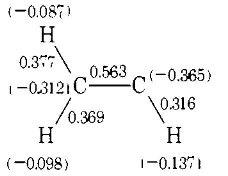

B. 4-31G Calculation at STO-3G Geometry (See Table V)

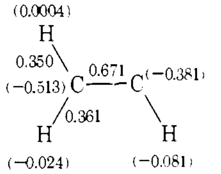

Scheme VI

A. STO-3G Calculation at STO-3G Geometry (See Table VI)

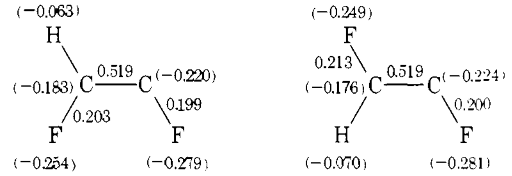

E_{rel}, kcal/mol	0.000	0.313
$N_T{}^{\pi}$	0.186 03	0.184 23
$P_{FF}{}^{\pi}$	0.000 01	0.000 00
$P_{FF}{}^{\sigma}$	0.000 00	0.000 00

B. 4-31G Calculation at STO-3G Geometry (See Table VI)

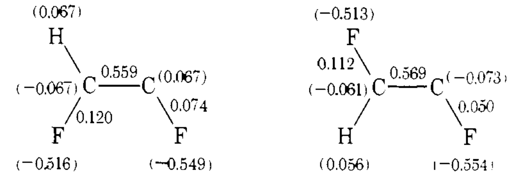

E_{rel}, kcal/mol	0.000	0.634
$N_T{}^{\pi}$	0.194 74	0.184 31
$P_{FF}{}^{\pi}$	0.000 26	0.000 00
$P_{FF}{}^{\sigma}$	0.000 62	0.000 06

D. CHX=CHX Molecules. We now consider the relative stability of the geometric isomers of $CHF{=}CHF$ molecules. The dominant σ conjugative interaction is $\sigma_{CH}-\sigma^*{}_{CX}$ which is maximized in the cis geometry. Accordingly, one expects that σ conjugative interactions will favor the cis isomer and that the two hydrogens in the cis isomer will be more positive than the

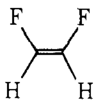

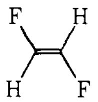

two hydrogens in the trans isomer. However, the ab initio calculations show exactly the opposite trend (Scheme VII) and, hence, we conclude that an electrostatic effect which minimizes the charge of the two hydrogens in the cis relative to the trans geometry is more important here than the σ conjugative effects.

Table XIII. Predicted Charges, Overlap Populations, and Relative Stability of the Geometric Isomers of CHF=CHF

Property	σ effect	Nonbonded effect	Electrostatic or steric effect	Ab initio	Exptl
H positive charge	Cis > trans		Trans > cis	Trans > cis	
F negative charge	Cis > trans	Trans > cis	Trans > cis	Trans > cis	
C-F overlap population	Trans > cis	Cis > trans	Trans > cis	Cis > trans[b]	
C-H overlap population	Trans > cis		Trans > cis		
C=C overlap population	Cis > trans	Trans > cis	Trans > cis	Trans > cis	
Relative stability	Cis > trans	Cis > trans	Trans > cis	Comparable	Cis > trans[a]

[a] See ref 27. [b] 4-31G basis set.

Table XIV. Predicted Geometric Parameters of the Geometric Isomers of HN=NH

Parameter	σ effect	Nonbonded effect	Electrostatic or steric effect	Ab initio	Exptl
r(N-N)	Trans > cis		Cis > trans	Trans > cis	
r(N-H)	Cis > trans		Cis > trans	Cis > trans	
∠HNN	Cis > trans		Cis > trans	Cis > trans	

Scheme VII

A. STO-3G Calculation at STO-3G Geometry (See Table IX)

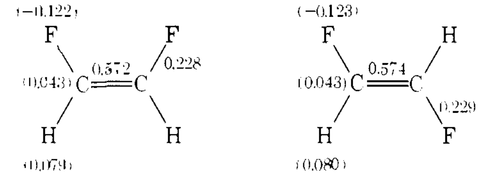

E_{rel}, kcal/mol	0.244	0.000
N_T^{π}	0.207 89	0.207 54
P_{FF}^{π}	0.000 01	0.000 00
P_{FF}^{σ}	0.000 01	0.000 00

B. 4-31G Calculation at STO-3G Geometry (See Table IX)

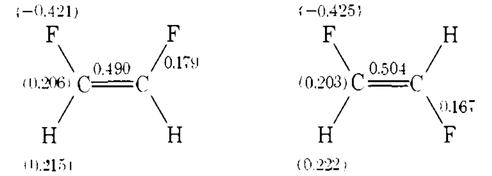

E_{rel}, kcal/mol	0.634	0.000
N_T^{π}	0.211 04	0.209 21
P_{FF}^{π}	0.000 23	0.000 01
P_{FF}^{σ}	0.000 46	0.000 07

C. 4-31G Calculation at 4-31G Geometry

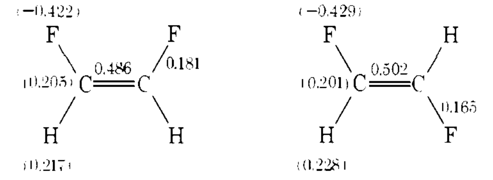

E_{rel}, kcal/mol	1.293	0.000
N_{tot}^{π}	0.215 40	0.212 57
P_{FF}^{π}	0.000 25	0.000 01
P_{FF}^{σ}	0.000 41	0.000 08

Accordingly, the greater stability of the cis isomer of CHF=CHF cannot be due to σ conjugative effects but rather some other effect, i.e., nonbonded attraction between the two F atoms.

The ab initio data for CHF=CHF are displayed in Scheme VII and the various predictions based on each of the three key effects previously discussed are outlined in Table XIII. Nonbonded attraction can account for all ab initio and experimental trends except the relative energy of the two isomers as calculated by either basis set. A recent calculation by Binkley and Pople at the 6-311G* level correctly predicted that *cis*-CHF=CHF is more stable than *trans*- by 0.260 kcal/mol.[28] The total π and long-range overlap populations of the geometric isomers of CHF=CHF provide further evidence of the dominance of nonbonded attractions and confirm our original analysis.[15]

Geometry of Molecules. A comparison of the geometries of related molecules can be useful in evaluating the relative importance of σ conjugation, nonbonded interactions, and electrostatic or steric effects. Specifically, these effects influence bond lengths and bond angles of geometric isomers in a predictable way.

n-σ^* and σ-σ^* σ conjugative effects have the following geometrical consequences, which will be accentuated in an anti geometrical arrangement of donor and acceptor bonds.

(a) Charge transfer from n to σ^* results in lengthening of the acceptor bond.

(b) Charge transfer from σ to σ^* results in lengthening of both donor and acceptor bonds.

Similarly, nonbonded X···X interaction in XYYX and XHY=YHX molecules have the following geometrical effects:

(a) Charge transfer from the antisymmetric X···X π or σ HOMO to the π or σ antibonding LUMO of the central bond fragment results in lengthening of the Y-Y bond and shortening of the Y-X bond in the cis isomer relative to the trans isomer.

The variation of geometrical parameters, a result of dipolar and steric effects, can be intuitively predicted.

A. R$\ddot{\text{N}}$=$\ddot{\text{N}}$R Systems. We first consider the case of the parent system HN=NH. The ab initio data of the STO-3G optimized geometries for HN=NH are displayed in Table III and predictions based on the above considerations are collected in Table XIV. Comparison of our ab initio results with the various predictions reveals that σ interactions are larger in the cis isomer since the N-N bond length varies in the order trans > cis.

In the case of N_2F_2, all three of the effects discussed previously obtain. Arguing as before, predictions concerning the $\ddot{\text{N}}$-$\ddot{\text{N}}$ and $\ddot{\text{N}}$-F bond length can be made on the basis of these effects (Table XV).

Ab initio and experimental data for *cis*- and *trans*-N_2F_2 are shown in Table IV and summarized in Table XV. Once again, the longer N-F bond length, as well as an experimentally determined shorter bond length in the cis isomer, is in line with a dominant n_N-σ^*_{NF} conjugative effect. It is interesting to note that the ab initio calculated N-N bond length trend, i.e., cis > trans, is opposite to what is found experimentally. The previously discussed $\ddot{\text{N}}$=$\ddot{\text{N}}$ overlap populations dependence upon basis set suggests that geometry optimization at the 4-31G level

Table XV. Predicted Geometrical Parameters of the Geometric Isomers of FN=NF

Parameter	σ effect	Nonbonded effect	Electrostatic or steric effect	Ab initio	Exptl[a]
r(N–N)	Trans > cis	Cis > trans	Cis > trans	Cis > trans	Trans > cis
r(N–F)	Cis > trans	Trans > cis	Cis > trans	Cis > trans	Cis > trans
∠FNN	Cis > trans	Trans > cis	Cis > trans	Cis > trans	Cis > trans

[a] See ref 29.

Table XVI. Predicted Geometrical Parameters of the Geometric Isomers of $F_bCH{=}\ddot{N}F_a$

Parameter	σ effect	Nonbonded effect	Electrostatic or steric effect	STO-3G	4-31G
r(C–N)	Cis > trans	Cis > trans	Cis > trans	Cis = Trans	Cis > trans
r(C–F_b)	Cis > trans	Trans > cis	Cis > trans	Cis > trans	Cis > trans
r(C–H)	Trans > cis			Trans > cis	Trans > cis
∠(F_bCN)	Cis > trans	Trans > cis	Cis > trans	Trans > cis	Cis > trans
∠(F_aNC)	Cis > trans	Trans > cis	Cis > trans	Cis > trans	Cis > trans

Table XVII. Predicted Geometric Parameters of the Geometric Isomers of $F_bCH{=}\bar{C}F_a$

Parameter	σ effect	Nonbonded effect	Electrostatic or steric effect	STO-3G
r(C–C)	Cis > trans	Cis > trans	Cis > trans	Cis > trans
r(C–F_b)	Cis > trans	Trans > cis	Cis > trans	Cis > trans
r(C–H)	Trans > cis			Trans > cis
∠F_bCC	Cis > trans	Trans > cis	Cis > trans	Cis > trans
∠F_aCC	Cis > trans	Trans > cis	Cis > trans	Cis > trans

Table XVIII. Predicted Geometrical Parameters of the Geometric Isomers of FHC=CHF

Parameter	σ effect	Nonbonded effect	Electrostatic or steric effect	Ab initio	Exptl[a]
r(C–C)	Trans > cis	Cis > trans	Cis > trans	Cis > trans	Cis > trans
r(C–F)	Cis > trans	Trans > cis	Cis > trans	Cis > trans	Trans > cis
r(C–H)	Cis > trans		Cis > trans		Cis > trans
∠FCC	Cis > trans	Trans > cis	Cis > trans	Cis > trans	Cis > trans
∠HCC	Cis > trans		Cis > trans	Trans > cis	Trans > cis

[a] See ref 30.

will be an improvement. Admittedly, the differences in geometrical parameters found between the cis and trans forms of N_2F_2 are small. Nevertheless, the data do suggest that the geometry of N_2F_2 is controlled to a large degree by σ conjugative effects.

B. RCH=N̈R Systems. The STO-3G optimized geometry of $H_2C{=}\ddot{N}H$ is presented in Table VII. If σ conjugative interactions are present, the C–H_c bond will be longer than the C–H_b bond; this is in agreement with the STO-3G computed results.

Predictions based on our analysis for the $HFC{=}\ddot{N}F$ systems are presented in Table XVI. The 4-31G and STO-3G optimized geometries for $HFC{=}\ddot{N}F$ are given in Table VIII and summarized in Table XVI. Although steric effects and σ conjugative effects go in the same direction, the fact that the C–H bond is elongated in the trans isomer suggests that σ conjugative effects are significant.

C. RCH=C̈R⁻ Systems. In the case of $H_2C{=}\ddot{C}H^-$, σ conjugative interactions will weaken the C–H bond which is anti to the lone pair on the adjacent carbon. This is also predicted by the STO-3G computation (Table V).

The STO-3G optimized geometry for the $FCH{=}\ddot{C}F^-$ geometrical isomers is presented in Table VI. A summary of these results along with the expected trends based on the various interactions within this molecule is given in Table XVII. Predictions based on steric effects again parallel those based on σ conjugative interactions. However, the longer C–H bond in the trans isomer again suggests the presence of σ conjugative effects.

D. FHC=CHF Systems. The variation of the geometrical parameters of *cis*- and *trans*-1,2-difluoroethylene can be predicted on the basis of the three previously discussed effects. These predictions are tabulated in Table XVI.

The results of ab initio calculations and experimental studies are collected in Table IX and summarized in Table XVIII. The longer cis C–C bond length as well as the shorter cis C–F bond length, as determined experimentally, strongly support our previous conclusion that nonbonded attraction between the two fluorine groups is the dominant factor controlling the geometry of this molecule.

An interesting trend found in all present or past calculations of geometric isomers is that the bond angles in cis and trans isomers always, with one exception, vary in a manner expected on the basis of σ conjugative effects as well as simple steric considerations.

Conclusion

The most important conclusions follow.

(1) Molecules can be viewed as composites of donor lone pairs and bonds and acceptor bonds. The preferred geometry of a molecule is the one which maximizes the interaction between the best donor lone pair or bond and best acceptor bond, if σ conjugative effects are not seriously counterbalanced by other effects.

(2) The orientation affording maximal n–σ^* and σ–σ^* interaction is the anti and not the syn, as one might intuitively have thought.

(3) σ conjugative interactions diminish in importance relative to X···X nonbonded attraction along the series XN═NX, XN═CHX, CHX═CHX. They can best be studied in systems like $CH_2{=}\dot{C}H$ and $CH_2{=}\ddot{C}H^-$ where nonbonded attractions and steric effects are not competing.

Hyperconjugation is an old idea.[31-36] Various authors have described how hyperconjugation can influence molecular geometry[37] but have confined their attention in comparisons of structures involving go vs. no-go hyperconjugation. A typical example is provided by the analysis of the conformational preference exhibited by hydrazine. In the gauche geometry, there is an n–σ^* interaction which vanishes at the cis or trans conformations. By contrast, we have focused attention on comparisons of structures where hyperconjugation might have been expected to be comparable, e.g., N_2F_2. There, we found that exactly the opposite situation obtains, i.e., syn vs. anti hyperconjugative stabilizations are different in magnitude with the anti always expected to dominate.

In previous papers,[15-20] we identified an electronic factor, tentatively termed nonbonded attraction, which favors crowded geometries (e.g., $C_2H_2F_2$). We have now seen that σ conjugative interactions may also prefer a crowded geometry (e.g., N_2F_2). Such interactions lead to charge redistribution which is unexpected intuitively, e.g., the fluorine atoms are more negative in *cis*- rather than *trans*-N_2F_2.

We wish to reemphasize a point which has been implicitly and/or explicitly discussed in this and previous works. Qualitative MO theory asserts its power in the prediction of trends rather than isolated events. Accordingly, a given σ conjugative interaction may be insignificant or significant depending upon the energy gap separating the interacting orbitals. Whenever weak interactions obtain, the preferred geometry of a molecule will be the one which minimizes overlap repulsion and Coulomb repulsion; i.e., in such cases steric effects prevail. An example is the conformational preference of ethane. In this case, σ_{CH}–σ^*_{CH} interactions are very weak and steric effects may dominate. This is borne out by the computational tests of Sovers et al.[38] Note, however, that even the σ_{CH}–σ^*_{CH} interactions dictate a minimum energy staggered conformation, i.e., in this case steric and σ conjugative effects work in the same direction, and determining which one dominates may be just an academic question. By contrast, whenever strong interactions obtain, deviations from steric control can be expected, e.g., N_2F_2.

The syn–anti overlap differentiation may have many important consequences for conformational analysis as well as chemical reactivity.[39] Extensions of the ideas presented in this paper to these areas will be forthcoming.

Acknowledgment. This work was made possible by a NATO Fellowship (N.D.E. and F.B.) and an A. P. Sloan Fellowship (N.D.E., 1976–1978).

References and Notes

(1) (a) University of Washington; (b) Universita di Bologna.
(2) M. J. S. Dewar, "The Molecular Orbital Theory of Organic Chemistry", McGraw-Hill, New York, N.Y., 1969.
(3) W. T. Borden, "Modern Molecular Orbital Theory for Organic Chemists", Prentice-Hall, Englewood Cliffs, N.J., 1975.
(4) (a) For a discussion of the relative importance of two electron-stabilizing and four electron-destabilizing interactions, see N. D. Epiotis and R. L. Yates, *J. Am. Chem. Soc.*, **98,** 461 (1976). (b) N. D. Epiotis, W. R. Cherry, S. Shaik, R. L. Yates, and F. Bernardi, *Top. Curr. Chem.*, **70,** (1977).
(5) R. Hoffmann, *Acc. Chem. Res.*, **4,** 1 (1971).
(6) W. T. Borden and W. L. Jorgensen, *J. Am. Chem. Soc.*, **95,** 6649 (1973).
(7) W. J. Hehre and L. Salem, *J. Chem. Soc., Chem. Commun.*, 754 (1973).
(8) The forms of the hybrid orbitals used in this work can be found in most quantum chemistry textbooks. For example, see W. Kauzmann, "Quantum Chemistry", Academic Press, New York, N.Y., 1957.
(9) The group orbitals of HN– were computed by the CNDO/2 method. For a discussion of this procedure, see J. A. Pople and D. L. Beveridge, "Approximate Molecular Orbital Theory", McGraw-Hill, New York, N.Y., 1970.
(10) K. Fukui, K. Morokuma, H. Kato, and T. Yonezawa, *Bull. Chem. Soc. Jpn.*, **36,** 217 (1963).
(11) J. March, "Advanced Organic Chemistry", McGraw-Hill, New York, N.Y., 1968.
(12) E. J. Fendler and J. H. Fendler, *Adv. Phys. Org. Chem.*, **7,** 229 (1970).
(13) H. Lund, *Acta Chem. Scand.*, **14,** 1927 (1960).
(14) W. L. Jorgensen and L. Salem, "The Organic Chemist's Book of Orbitals", Academic Press, New York, N.Y., 1973.
(15) N. D. Epiotis, *J. Am. Chem. Soc.*, **95,** 3087 (1973).
(16) N. D. Epiotis and W. Cherry, *J. Chem. Soc., Chem. Commun.*, 278 (1973).
(17) N. D. Epiotis, D. Bjorkquist, L. Bjorkquist, and S. Sarkanen, *J. Am. Chem. Soc.*, **95,** 7558 (1973).
(18) N. D. Epiotis, S. Sarkanen, D. Bjorkquist, J. Bjorkquist, and R. Yates, *J. Am. Chem. Soc.*, **96,** 4075 (1974).
(19) N. D. Epiotis, R. L. Yates, and F. Bernardi, *J. Am. Chem. Soc.*, **97,** 5961 (1975).
(20) N. D. Epiotis, R. L. Yates, F. Bernardi, and H. B. Schlegel, *J. Am. Chem. Soc.*, **98,** 2385 (1976).
(21) W. J. Hehre, W. A. Lathan, R. Ditchfield, M. D. Newton, and J. A. Pople, Quantum Chemistry Program Exchange, No. 236, Indiana University, Bloomington, Ind.
(22) W. J. Hehre, R. F. Stewart, and J. A. Pople, *J. Chem. Phys.*, **51,** 2657 (1969).
(23) R. Ditchfield, W. J. Hehre, and J. A. Pople, *J. Chem. Phys.*, **54,** 724 (1971).
(24) (a) For another recent calculation on N_2H_2 see R. Ahlrichs and V. Staemmler, *Chem. Phys. Lett.*, **37,** 77 (1976). (b) A referee has kindly informed us that geometry optimization at the 4-31G level gives the cis isomer of N_2F_2 more stable than the trans isomer by 1.047 kcal/mol.
(25) R. K. Bohn and S. H. Bauer, *Inorg. Chem.*, **6,** 309 (1967).
(26) J. M. Howell and L. J. Kirschenbaum, private communication.
(27) In a recent publication [J. M. Howell, *J. Am. Chem. Soc.*, **98,** 886 (1976)] Howell discussed cis–trans isomers of diazenes and substituted methyleneimides. This author noted the charge effects which we have discussed. He was hesitant to attribute them to σ conjugative effects, although he did suggest this possibility. For example, the author stated ". . . we are hesitant to accept hyperconjugation as the sole, decisive factor in determining the energies of different isomers. If hyperconjugation were dominant, we would expect the C═N overlap population would be higher and the bond length shorter in

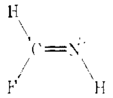

than in

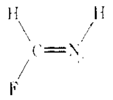

and in *cis*-FHC═N̈F than in *trans*-FHC═N̈F." However, we have seen that nonbonded attraction dominates σ conjugative effects in the latter two molecules. In short, our demonstration of some key algebraic relationships which renders anti superior to syn n–σ^* overlap, coupled with the realization of the importance of nonbonded attractive effects, may well remove any hesitancy to accept the importance of σ conjugation.
(28) J. S. Binkley and J. A. Pople, *Chem. Phys. Lett.*, **45,** 197 (1977).
(29) H. G. Viehe, *Chem. Ber.*, **93,** 1697 (1960); E. B. Whipple, W. E. Stewart, G. S. Reddy, and J. H. Goldstein, *J. Chem. Phys.*, **34,** 2136 (1961).
(30) J. L. Carlos, Jr., R. R. Karl, Jr., and S. H. Bauer, *J. Chem. Soc., Faraday Trans. 2*, **70,** 177 (1974).
(31) G. W. Wheland, *J. Chem. Phys.*, **2,** 474 (1934).
(32) L. Pauling, H. S. Springall, and K. J. Palmer, *J. Am. Chem. Soc.*, **61,** 927 (1939).
(33) R. S. Mulliken, *J. Chem. Phys.*, **7,** 339 (1939).
(34) R. S. Mulliken, C. A. Rieke, and W. G. Brown, *J. Am. Chem. Soc.*, **63,** 41 (1941).
(35) J. W. Baker and W. S. Nathan, *J. Chem. Soc.*, 1844 (1935).
(36) M. J. S. Dewar, "Hyperconjugation", Ronald Press, New York, N.Y., 1962.
(37) L. Radom, J. A. Pople, and P. v. R. Schleyer, *J. Am. Chem. Soc.*, **94,** 5925 (1972); L. Radom, J. A. Pople, V. Buss, and P. v. R. Schleyer, *ibid.*, **92,** 6380, 6987 (1970); L. Radom, W. J. Hehre, and J. A. Pople, *ibid.*, **94,** 2371 (1972); S. David, O. Eisenstein, W. J. Hehre, L. Salem, and R. Hoffmann, *ibid.*, **95,** 3806 (1973); R. Hoffmann, L. Radom, J. A. Pople, P. v. R. Schleyer, W. J. Hehre, and L. Salem, *ibid.*, **94,** 6221 (1972).
(38) O. J. Sovers, C. W. Kern, R. M. Pitzer, and M. Karplus, *J. Chem. Phys.*, **49,** 2592 (1968).
(39) P. Deslongchamps, *Tetrahedron*, **31,** 2463 (1975); E. L. Eliel and F. W. Nader, *J. Am. Chem. Soc.*, **92,** 584 (1970); J. M. Lehn, G. Wipff, and H. B. Bürgi, *Helv. Chim. Acta*, **57,** 493 (1974); H. B. Bürgi, J. M. Lehn, and G. Wipff, *J. Am. Chem. Soc.*, **96,** 1956 (1974); J. M. Lehn and G. Wipff, *ibid.*, **96,** 4048 (1974); H. B. Bürgi, J. D. Dunitz, J. M. Lehn, and G. Wipff, *Tetrahedron*, **30,** 1563 (1974).